Proceedings of the 18th International Symposium on the Packaging and Transportation of Radioactive Materials
PATRAM 2016
September 18-23, 2016, Kobe, Japan

Paper No. 2039

Cross Code Verification of a Thermal Stress Analysis of a Thin Walled RAM Transport Package during and after a Regulatory Pool Fire

Author Andy Cummings
Affiliation International Nuclear Services

Abstract

Finite Element Analysis (FEA) is an effective tool for assessing packages used to transport Radioactive Materials (RAM) in normal operation and in extreme, hypothetical accident conditions. RAM transport packages must satisfy the requirements of the IAEA Regulations by demonstrating their performance in a series of tests including a 9m drop onto an unyielding target and a subsequent 30 minute pool fire with a flame temperature of 800°C. Sufficient performance of a RAM transport package in an accident is determined by its ability to maintain a containment boundary in any impact or fire scenario and to withstand the cumulative effects of an impact followed by a fire.

In this paper a thin walled package, consisting of three concentric shells, has been assessed to determine which shell is most likely to fail as a result of a thermal accident. The package utilises a polymeric neutron shielding material between the concentric shells which may exceed its degradation temperature during the fire and begin to off-gas, thereby generating pressure. The analysis considers the combined effects of thermal expansion and internal pressure acting on the inner and outer shell during the fire transient and a subsequent cool down period.

The problem has been solved in two analysis codes, Abaqus and LS DYNA to cross-verify the results. This paper discusses the merits and limitations of both Finite Element Codes when used for solving sequentially-coupled thermal stress problems.

Introduction

The M4-12 package utilises a cross-linked polyethylene as a neutron shielding material, commercially referred to as Vitrite. **Figure 1** shows the package body construction consisting of three concentric, duplex stainless steel shells (6mm thick) welded to a large lid end forging and a base plate. The two, empty cylindrical volumes between the shells are infilled with Vitrite, housed in 30 aluminium extrusions of 3mm wall thickness, see inset of **Figure 1**. Previous work demonstrated that temperatures exceeding 390°C will cause the Vitrite to degrade **[1]**. The degradation process causes off-gassing which may increase the internal pressure within the cavity that houses the neutron shielding material **[2]**.

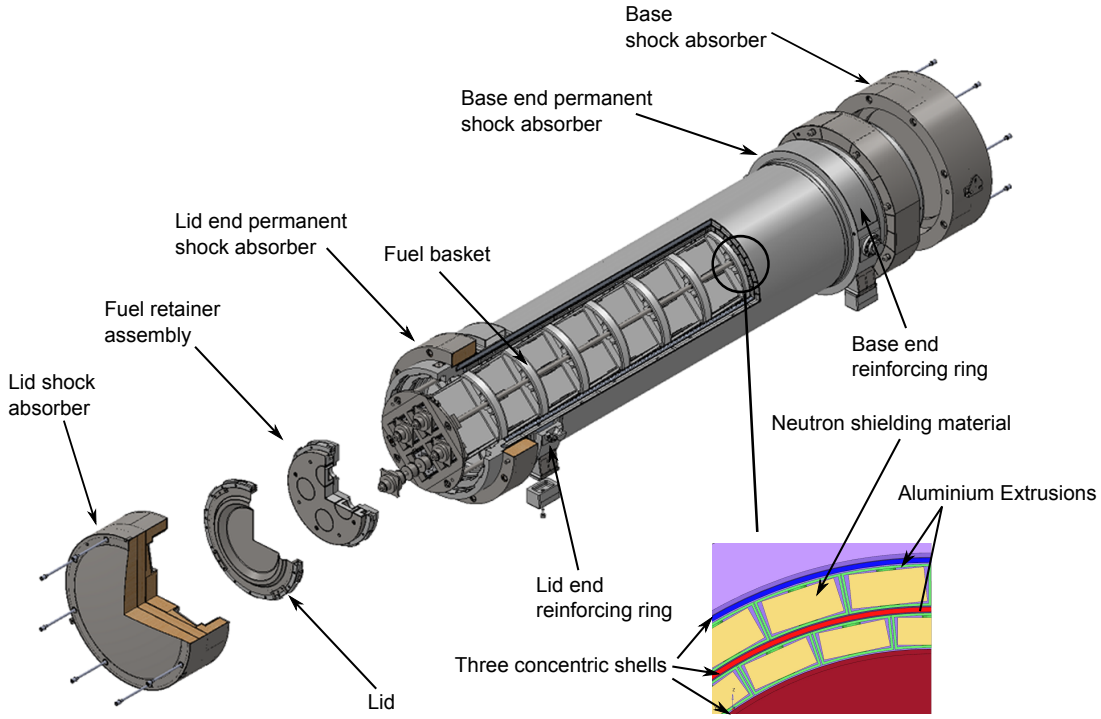

Figure 1: A Schematic of the M4-12 RAM Transport Package

Eight fusible plugs in the outer shell are designed to fail during a fire and provide a sufficient path for the gas to escape preventing over-pressurisation. Because the time duration and amount of off-gassing is variable depending on the package initial conditions there was a concern that the fusible plugs were not sufficiently sized or optimally positioned to vent the gas from the package. The purpose of this study was to assess the behaviour of the inner and outer shells under

combined thermal and pressure loading, in order to determine whether a containment boundary breach was possible due to a thermal accident. Four possible outcomes were identified:-

1. Inner shell failure, containment boundary breach
2. Inner and outer shell failure, containment boundary breach
3. Outer shell failure, pressure vented, containment boundary intact
4. Inner and outer shell remain intact, containment boundary intact

This paper presents a Finite Element methodology to determine which of these outcomes is possible.

Modelling Approach

For transient thermal stress problems there are two approaches possible to obtain a solution; a sequentially coupled approach or a fully coupled, temperature-displacement analysis. The sequentially coupled method consists of carrying out a heat transfer analysis first to calculate a temperature profile throughout the transient. This is followed by a structural analysis where the previously calculated temperatures are mapped onto a structural model that expands producing thermal strains. In the fully coupled approach only one model is used to calculate both temperatures and displacements simultaneously. One key benefit to this approach is that it more accurately models thermal contact accounting for changing gap sizes between the shells, extrusions and shielding material due to thermal expansion. The main disadvantage is that all of the structural interactions between non-structural parts has to be solved, increasing model complexity significantly.

Preliminary runs indicated that the thin walled steel shells buckled due to thermal expansion and pressure within the cavity which resulted in some material plasticity. Obtaining solutions for buckling and post-buckling response with FEA can be very challenging, therefore a simplified solution was sought with a sequentially coupled modelling approach.

The problem was solved in two different FEA codes; Abaqus and LS DYNA. This built confidence in the approach and served as preliminary verification. It also enabled a sufficiently wide range of sensitivity studies by taking advantage of the different solution techniques available within both codes. Both explicit and implicit methods were used to find solutions, the main difference being that the explicit analyses were run in time durations much smaller than the fire

and cooling phase but large enough for the solutions to remain quasi-static. To ensure dynamic effects were not present the internal and kinetic energy time histories were monitored throughout the solution. For a quasi-static solution method the Abaqus Users Manual **[3]** recommends that the kinetic energy is 5% - 10% of the internal energy. The explicit solution results were also benchmarked against implicit results. In LS DYNA the ability to switch between implicit and explicit methods to step through the solution was also explored.

Mesh

The heat transfer and thermal stress models were constructed entirely of brick elements, **Figure 2**. The design involves thin walled shells (6mm) that lend themselves to a shell element mesh, however the shells are butt-welded to a much heavier lid forging, a thick base plate (20mm) and 2 x forged reinforcing rings used to support the trunnions in handling operations. To expedite the solution hexahedral elements were used.

D3C3D8 diffusive heat transfer elements were assigned to the Abaqus thermal model **[3]**. Three dimensional, 8-node, brick elements for heat transfer were also used for the LS DYNA model **[4]**. In the structural models selective reduced integration element formulation, ELFORM=2 was used in LS DYNA and C3D8 linear brick elements were used in Abaqus.

Material Modelling

The heat transfer calculations were carried out using materials data from various sources **[5–10]**. A “conduction” model was applied to Vitrite, meaning that the predicted Vitrite temperatures may be in excess of 390°C i.e. not accounting for thermal degradation.

Thermal expansion coefficients for the steels were taken from **[5]**. The anticipated response of the Duplex stainless steel (1.4462) shells at elevated temperatures was elastic-plastic. **Figure 3a** shows true stress true strain data for the Duplex stainless steel applied to the shells which accounted for variations in the material response throughout the predicted temperature range **[10]**. Chen *et al.* **[10]** provided a conservative, temperature dependent yield stress and failure strain definition, **Figure 3b**. The failure strain was taken as the ultimate or necking strain at each temperature.

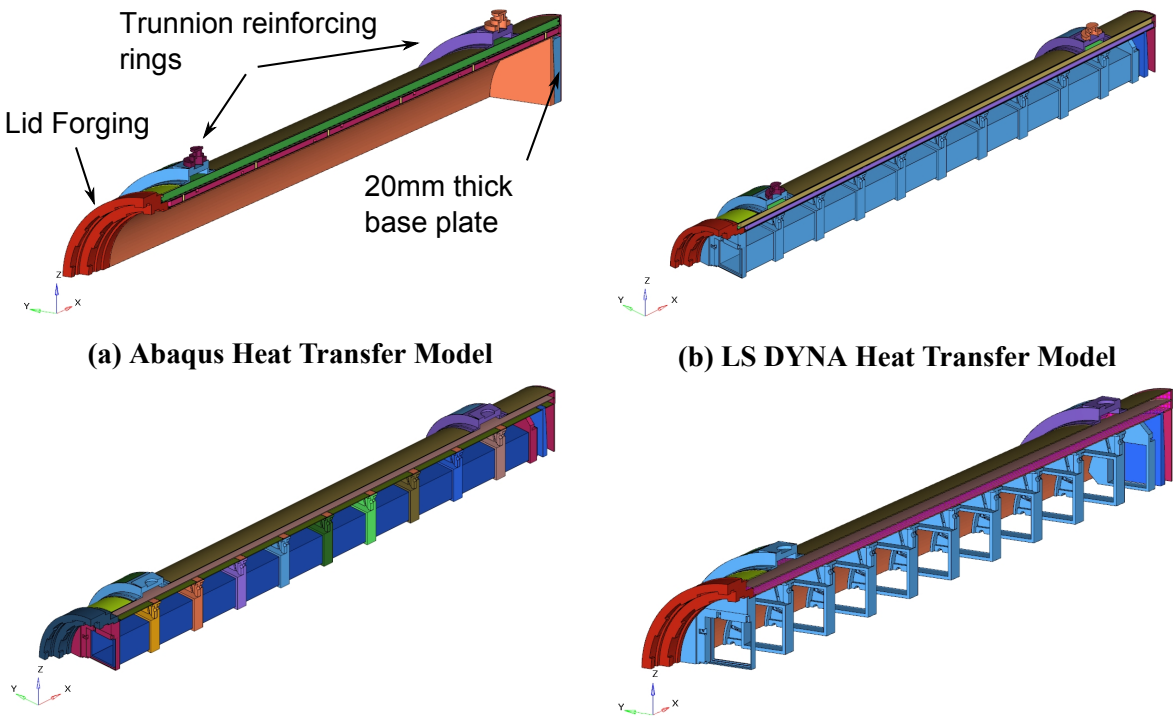

(a) Abaqus Heat Transfer Model

(b) LS DYNA Heat Transfer Model

(c) Abaqus Thermal Stress Model

(d) LS DYNA Thermal Stress Model

Figure 2: Finite Element Models used in the Simulations

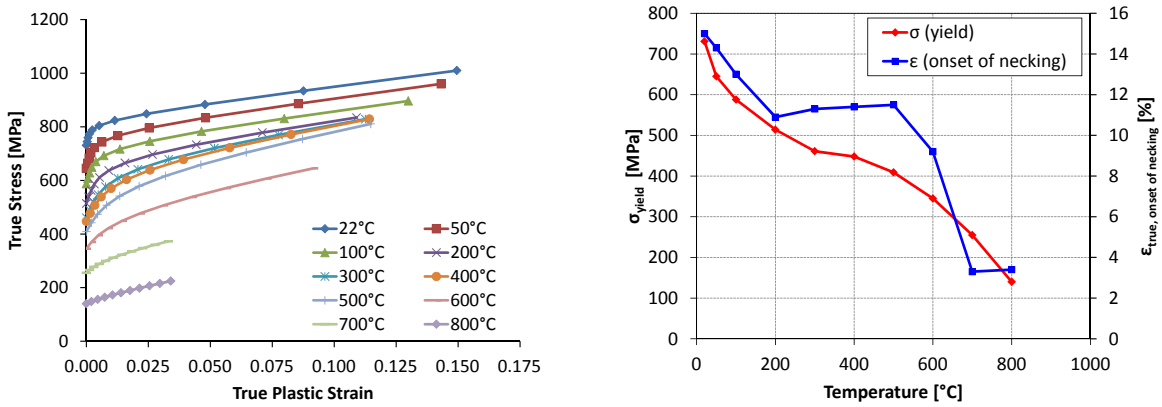

(a) True Stress-Strain Curves at Elevated Temperatures Derived from Published Data *after* Chen *et al.*

(b) Temperature Dependant True Ultimate Strain and Yield Stress from Published Data *after* Chen *et al.*

Figure 3: Mechanical Properties of Duplex Stainless Steel

Boundary Conditions - Heat Transfer

In both LS DYNA and Abaqus a quadrant of the M4-12 was modelled. In the heat transfer analysis the symmetry boundaries were assumed to be adiabatic, meaning that no heat can transfer to or from those surfaces. Convection and radiation were applied to all external surfaces as described in **[11]** to predict temperatures during normal and accident conditions of transport. The surfaces underneath each shock absorber were assumed to be adiabatic, mitigating the need to include the shock absorbers in the model.

In the Abaqus model the normal conditions of transport (NCT), the regulatory 30 minute fire and subsequent cool-down period were modelled in three discrete steps; one steady-state step followed by two transient steps. In each step the convection and radiation boundary conditions were changed appropriately.

In LS DYNA the full fire and cooling sequence was achieved by a preliminary steady-state analysis for NCT and then using the calculated nodal temperatures as an initial condition for a single transient heat transfer analysis. During this second analysis the changeover at the end of the fire to the cooldown phase was handled by time and temperature dependent load curves.

The heat load from the nuclear fuel was applied as a heat flux. The fuel basket was modelled for the heat transfer analysis carried out in LS DYNA and the flux applied to the inner walls of the fuel lodgements. This was to allow for its easy inclusion in the subsequent thermal stress run and is necessary because the basket provides a supporting structure to the inner shell. This is discussed further in the next section.

However in Abaqus the fuel basket was not modelled, and a heat flux was applied to bands of the inner shell where the fuel basket ribs were assumed to be perfectly conducting with the inner shell. This constitutes one of the more significant differences in approach between the two models.

Output was requested at 100 evenly spaced time points throughout the fire and a further 100 evenly spaced time points throughout the cooling phase. This was achieved by setting *OUTPUT, NUMBER INTERVAL = 99 in Abaqus. In LS DYNA the output frequency was controlled by controlling the minimum time step of the solution with a load curve for each phase (fire and cooling) and the d3plot output interval was set to a very small number.

Boundary Conditions - Thermal Stress

In both codes the structural models were fixed at the lid end forging which is very stiff in relation to the rest of the package. The symmetry boundary conditions were applied by eliminating appropriate degrees of freedom of the nodes on each symmetry plane.

The structural models were loaded with the preceding heat transfer results. Both LS DYNA and Abaqus apply nodal temperatures to the structural elements integration points (using numerical integration) at every time step during the analysis. Both FEA codes use linear interpolation to calculate intermediate temperature values between time steps.

The fuel basket was modelled as an iso-thermal rigid body. In LS DYNA the nodal temperatures from the preceding heat transfer analysis were over-ridden for the fuel basket by the application of a *MAT_RIGID material definition. This means that the internal fuel basket does not expand due to elevated temperature or deform due to pressure acting on the inner shell, which is considered a pessimism as the basket will essentially act as a die to the inner shell. The basket was modelled in the heat transfer analysis because introducing it later in the thermal stress analysis resulted in incorrectly mapped temperatures. This was a workaround solution as spatial interpolation of temperatures between dissimilar thermal and structural meshes was not achieved in LS DYNA.

In Abaqus the additional nodes and elements for the fuel basket were added into the thermal stress model and the difference between the heat transfer and structural mesh was handled by the keyword *TEMPERATURE, INTERPOLATE. Again the fuel basket was modelled as an iso-thermal rigid body.

Additionally the aluminium extrusions and Vitrite were removed from the thermal stress model (in both codes). This was a modelling assumption as both were considered non-structural at the predicted elevated temperatures.

Output of the thermal stress results was requested at twenty evenly spaced points throughout the thirty minute fire and a further twenty evenly spaced points throughout the cooling phase.

Sensitivity Analysis

The key unknown in the heat transfer model was the size of the gaps between the shells and the aluminium extrusions and Vitrite. This is complicated by thermal expansion, which means that any initial gaps would change throughout the fire and cooldown, affecting the heat transfer across the gaps and ultimately the temperature profile of the inner and outer shells. In the Abaqus model nominal dimensions of the shells and extrusions have been assumed and the position of the extrusions adjusted to fit equidistant between the shells, see **Figure 4**. In the LS DYNA model nominal dimensions of the shells have been assumed and the extrusions' positioning has been set irregularly but within allowable dimensional tolerancing. The gap sizes for the Abaqus model are annotated in **Figure 4** and those resulting from the LS DYNA model are shown in brackets.

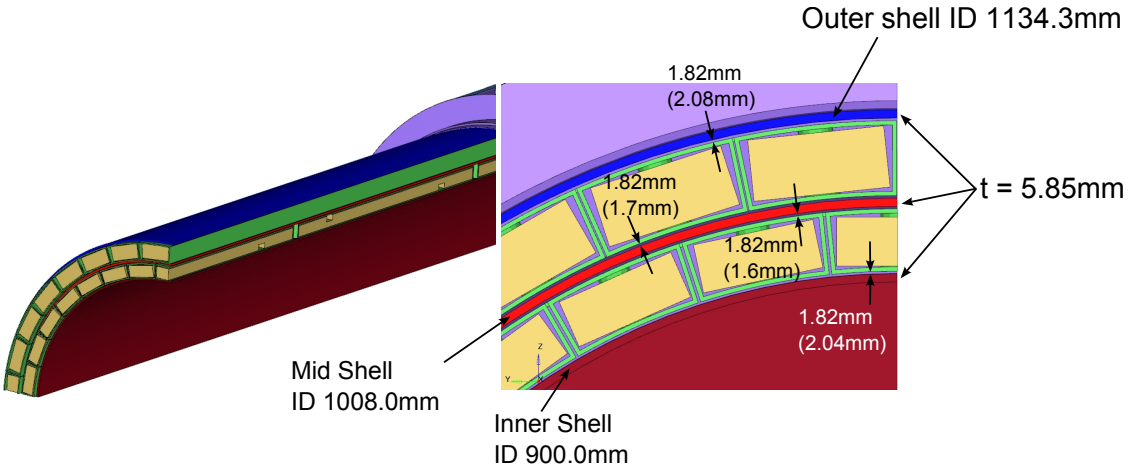

Figure 4: Initial Geometric Configuration of Heat Transfer Models (LS DYNA Gaps quoted in Brackets)

In the thermal stress analysis there were considered to be three significant unknown parameters:-

1. Pressure rise time
2. Magnitude of internal pressure
3. Presence of imperfections in shells

The pressure loading was assessed in a simple way. Firstly, the rise time was assumed to linearly increase until the end of the fire and then remain constant (i.e. the fusible plugs all fail

to activate). This is considered pessimistic because in reality the pressure would decrease as the temperature decreased during cooling. Also the predicted metal temperatures of the outer shell occur at the end of the fire and for the inner shell they occur sometime later[1]. Maintaining a constant pressure as the inner shell heats up is therefore considered a conservative assumption.

Note the predicted Vitrite peak temperatures occurred at the end of the fire and the model indicated that the Vitrite would off-gas for no more than one hour. The magnitude of pressure was increased in a series of runs from 25 barg to 80 barg. In this paper the results of the 25 barg case only are presented as solutions in both codes were not achieved up to 80 barg.

Imperfections in the shells also cause a difference in post-buckling response. Initially the model was run with no imperfections. Later imperfections were added which caused non-convergence using implicit solution methods. So to evaluate shell imperfection first a benchmarking explicit solution was performed for perfect shells. From this benchmark the explicit solution method was used to vary the imperfections in both shells.

The addition of imperfections was carried out only in Abaqus because the code offered the capability to compress a 3 hour period ($^1/_2$ hour fire and $2^1/_2$ hour cooling) into a much shorter time frame suitable for an explicit solution. Therefore results including imperfections are not discussed further in this paper.

Contact Modelling - Heat Transfer

The modelling of thermal contact resistance across the gaps between the shells, aluminium extrusions and Vitrite affected the predicted temperatures of the inner and outer shell. In both codes heat transfer by conductance and radiation was modelled. The application of the thermal contact resistance varied slightly between LS DYNA and Abaqus.

In Abaqus, thermal contact resistance was modelled across the gaps between the shells and the aluminium extrusions, **Figure 5a**. Gap conductance was modelled by applying temperature and gap dependant conductance values derived from **[13]**. Radiation was applied by assuming the shells were infinite concentric cylinders, each viewfactor set to 1 and the appropriate surface emissivity value assigned to each surface.

[1] The time at which the peak temperature of the inner shell was predicted was sensitive to the assumptions made for the thermal contact resistance across the internal gaps

In LS DYNA the thermal contact resistance model was applied to all contacting surfaces. This served as a sensitivity study, the differences between each model were ultimately judged by the structural response of the inner and outer shells to the temperature profile. Gap conductance was applied using a temperature independent, averaged conductance value that varied with gap distance. **Figure 5b** illustrates the difference in implementation of thermal gap conductance between the two codes. Radiation was handled by LS DYNA in a similar manner to Abaqus but all units were specified in Kelvin rather than °C.

Contact Modelling - Thermal Stress

In the structural assessment the only contact possible was between the inner shell and fuel basket. This was modelled in Abaqus and LS DYNA using general, single surface contact definitions and an assumed coefficient of friction $\mu = 0.3$, was applied. A typical value for metal to metal contact is $\mu = 0.2$, this has been increased slightly assuming that an increase in temperature will result in a marginally higher value **[14]**.

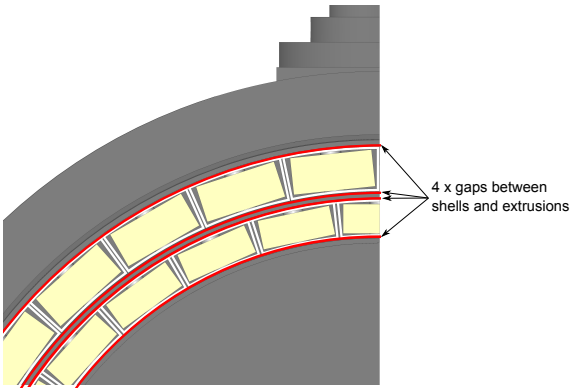

(a) Gaps in Abaqus Model where Thermal Contact Resistance was applied

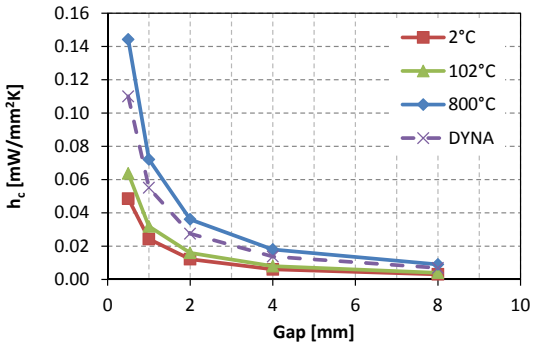

(b) Difference in Gap Conductance Models (Abaqus input as temperature dependant curves 2°C, 102°C and 800°C)

Figure 5: Thermal Contact Resistance

Solution Methods

The heat transfer analysis was completed with relative ease in both codes. The thermal stress analysis proved to be more difficult to obtain solutions consistently. The crux of the problem is due to geometric non-linearity. As the thin walled shells buckle, they ”snap-through” from one

geometrically load carrying state to another, **Figure 6**. At the point of snap-through the stiffness of the shell reduces to zero momentarily which can cause non-convergence of implicit solvers using iterative Newton Methods. The static method available in LS DYNA and Abaqus to solve this class of problem is the Riks Method (arc length), however this technique does not always step through time monotonically (i.e. valid solution can end at negative time states) so transient temperature mapping is not available.

The following equations provide a framework for a short discussion on the different solution methods available to tackle the problem **[15]**:-

$$\{F\} = [K]\{u\} \tag{1}$$

$$\{F\} = [K]\{u\} + [B]\{\dot{u}\} \tag{2}$$

$$\{F\} = [K]\{u\} + [B]\{\dot{u}\} + [M]\{\ddot{u}\} \tag{3}$$

$$[M]\{\ddot{u}\} = \{F_{external}\} - \{F_{internal}\} \tag{4}$$

Ideally the analysis would be solved pseudo-statically, solving equation 1 and using a time-stepping solution method throughout the fire and cooling period. However due to buckling of the inner and outer shells the solver often failed to converge. Addition of artificial damping with equation 2 helped the problem but did not always result in a converged solution.

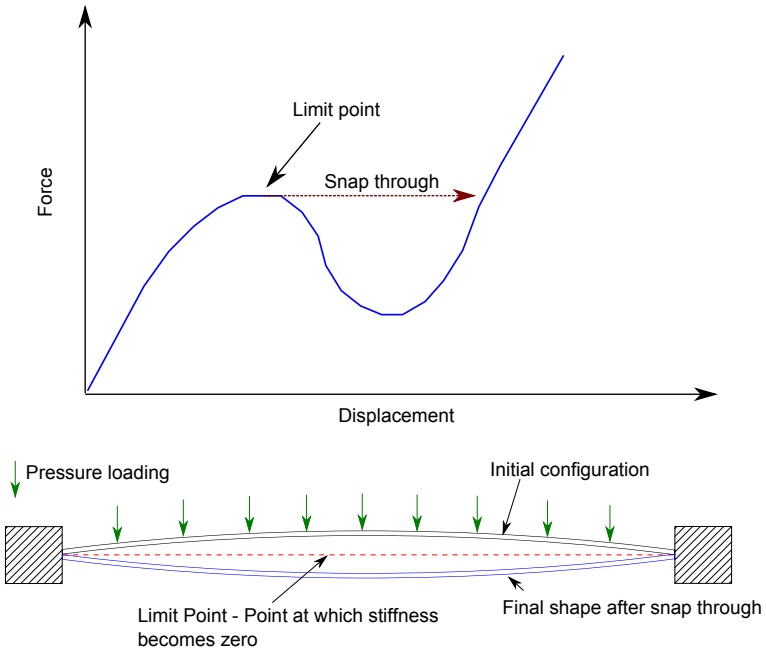

Figure 6: An Example of Geometric Non-Linearity and the Associated Force-Displacement Behaviour of a Structure that "Snaps-Through"

Running in the same time base as the preceding heat transfer analysis and solving equation 3 with an implicit dynamic method proved to be a more reliable way for obtaining many of the results. This stabilised the solution with the addition of real inertial effects and default, numerical damping coefficients **[3]**.

However the inclusion of imperfections to the shells meant that many of the runs failed even with the implicit dynamic approach. So to complete the study Abaqus/Explicit was used which solves equation 4. This has the computational benefit of carrying out element-wise calculations as opposed to building large matrices. However the method is limited to very small time steps to maintain numerical stability. To achieve pragmatic run times (overnight) the heat transfer results were compressed to a time duration that maintained a quasi-static solution. No "in-built" way of compressing the time base of the heat transfer results from LS DYNA was found, so for the purposes of robust verification the final runs were all carried out with just Abaqus.

Results

Heat Transfer - Temperature Profile

All post-processing was carried out in the third party software tool Hyperview part of the Hyperwork software bundle **[16]**. **Figure 7** shows the NCT temperature contour plots of the M4-12 quadrant model solved in both codes. Considering the difference in approach taken to modelling thermal contact, qualitative comparison is good. In both models the lid forging temperatures are over-predicted due to the simplistic approach to modelling this area.

Many of the lid end components that exist in the design have been omitted in these models and the heat load from the fuel has been applied as a flux directly to the forging in the Abaqus model. The LS DYNA model is a closer approximation because the fuel basket and thermal contact resistance between the basket and forging is modelled, however other components that would provide resistance to heat flow such as the lid and PWR retainer (Vitrite clad in steel) are not included. These modelling assumptions add pessimism to the initial conditions of the inner shell which is subsequently slightly hotter than it would be, particularly at the lid end. This approach would not be sufficient for a lid seal temperature analysis but is conservative for the structural assessment of the inner shell.

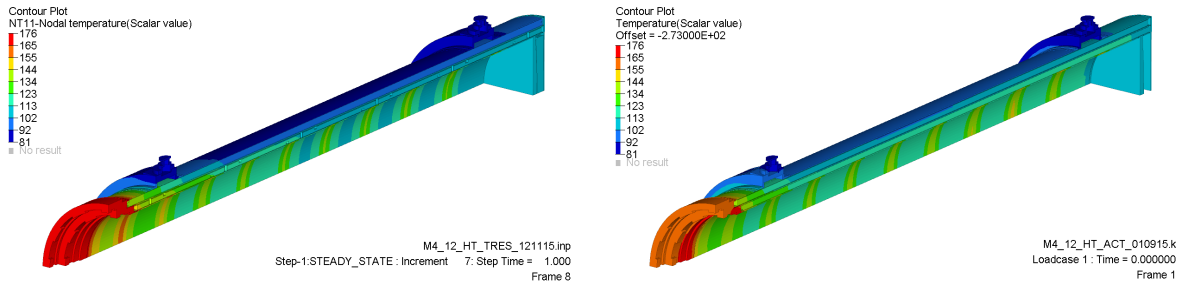

(a) Abaqus **(b) LS DYNA**

Figure 7: Heat Transfer Results for Normal Conditions of Transport

Figure 8 shows temperature contour plots of the M4-12 at the end of a regulatory 30 minute pool fire. Again the comparison of the results indicates that the temperature profiles are very similar. The effect of higher thermal contact resistance in the LS DYNA model is apparent through the wall thickness, where the outer extrusions and Vitrite are slightly cooler than those in the Abaqus model.

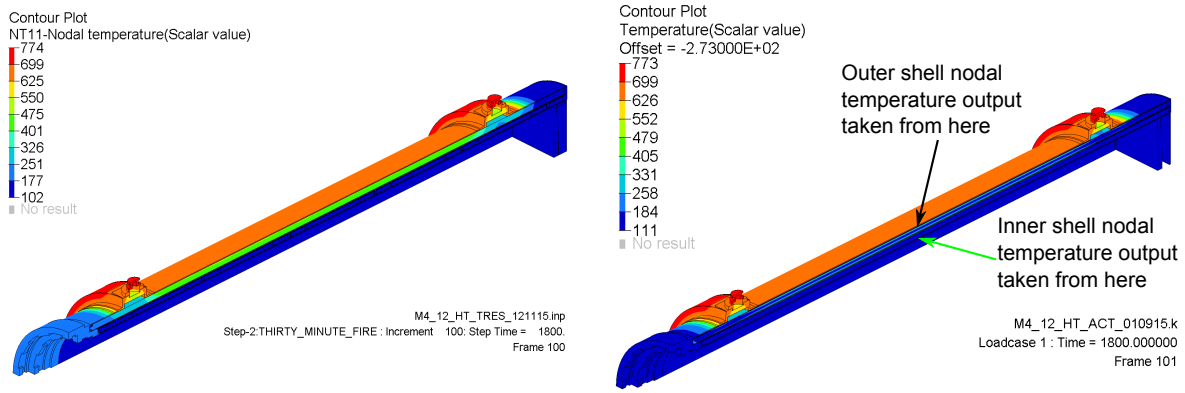

(a) Abaqus **(b) LS DYNA**

Figure 8: Heat Transfer Results for Accident Conditions of Transport

Figure 9 shows temperature time histories from nodes from both models located at the longitudinal mid-point of the inner and outer shells, the node locations are shown in **Figure 8b**. The curves indicate that the differences in contact modelling result in similar but not identical transient temperature results for the outer and inner shells. **Figure 9a** shows that the outer shell peak temperature is consistently predicted between analysis code irrespective of the modelling differences. The LS DYNA model cools more rapidly but both models converge to a similar steady state temperature.

Figure 9b shows that there is a bigger difference between the inner shell temperatures. Initially the LS DYNA model predicts slightly higher inner shell temperatures (12°C) than the Abaqus model. After an hour the Abaqus model inner shell gains slightly more heat than the LS DYNA model resulting in a hotter temperature by 36°C. This is attributed to three factors:-

1. Thermal contact resistance applied to aluminium extrusions and Vitrite in LS DYNA model (whereas in the Abaqus model they are assumed to be perfectly conducting).
2. The differences in implementation of the gap conductance model.
3. The difference in gaps sizes between the models.

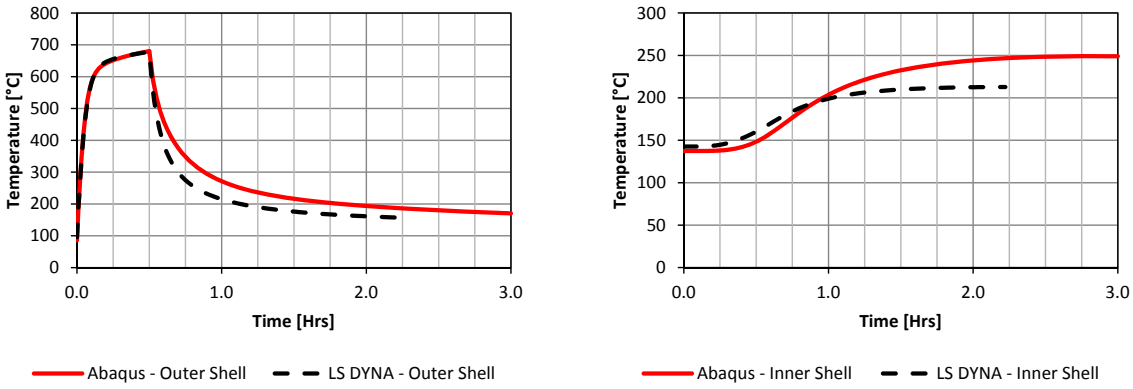

(a) Outer Shell **(b) Inner Shell**

Figure 9: Temperature Time Histories from Nodal Position at the Longitudinal Centre of the Shells during Accident Conditions of Transport

The main conclusion from this preliminary assessment was that the inner shell temperature is sensitive to changes to the internal gaps within the package, which are difficult to define initially due to geometric tolerancing and the number of components. They also change throughout the fire. In **[12]** a bounding case was used to assess this. In this heat transfer study it was also concluded that both codes were capable of adequately solving the thermal aspects of this problem; the results of the Abaqus model were benchmarked against previous PDSR thermal analysis and compared favourably.

Thermal Stress - Deformation

Figure 10 shows the resulting deformation after 30 minutes in the pool fire. The contour plots indicate that the entire package response is dominated by longitudinal thermal expansion. The Abaqus model resulted in a maximum of 34mm expansion, whereas the LS DYNA model resulted in a maximum of 28mm expansion.

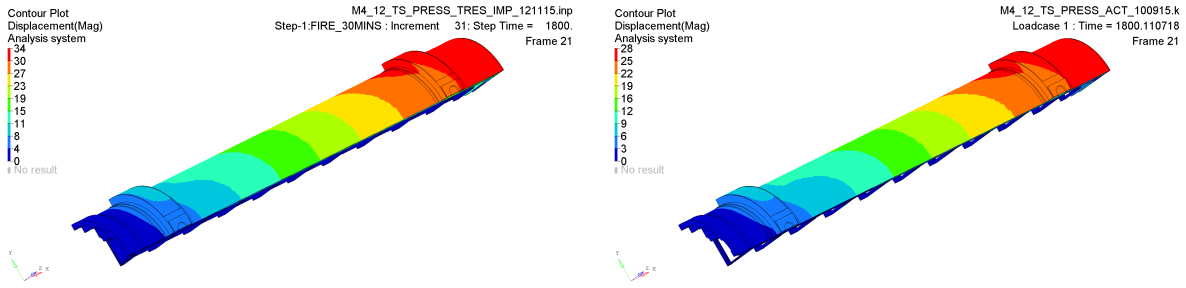

(a) Abaqus **(b) LS DYNA**

Figure 10: Displacement Contour Plots of the M4-12 at the end of 30 minute Regulatory Pool Fire

Thermal Stress - Strain Analysis

The largest plastic strains were found in the mid shell to base plate weld, **Figure 11**. The Abaqus model predicted 16.3% plastic strain and the LS DYNA model predicted 15.9% in this weld at the end of the fire. These strains increased to 24.0% (Abaqus) and 20.2% (LS DYNA) after 2 hours ($1^1/_2$ hour cooling period)[2]. It is evident that the magnitude of plastic strains is very similar between the models at the end of the fire. The difference in strains after 2 hours is attributed to the difference in temperature profile calculated by the preceding heat transfer results.

LS DYNA predicts the strain in the outer shell to base plate weld is 3.8% after the fire and after the cooldown increases to 6.3%. In comparison Abaqus predicts the strain in the outer shell to base plate weld is also 3.8% after the fire and at the end of the cooldown increases to 7.1%. As these strains occur at a weld they are considered relatively large; mesh refinement would cause them to increase. Therefore they may result in weld failure causing a release of internal pressure and preventing a containment boundary breach.

The predicted plastic strain in the inner shell to base plate weld was 4.0% (Abaqus) and 4.2% (LS DYNA) at the end of the cooling period. Failure here is less likely as the magnitude of strain is lower (much lower in the case of the mid shell welded joint). A failure of this weld would be acceptable because it is not part of the containment boundary. However it would not be beneficial as it would not provide a path for the excess gas to release pressure. These strains

[2]The results averaging used in comparing these values is equivalent between the codes. In both instances element integration point values have been averaged to provide element centroidal values, nodal averaging has been applied to produce the contour plot but the reported maximum values in the legend result from centroidal values.

are caused by the ΔT across the total package wall which causes rotation of the base plate due to a greater rate of longitudinal expansion of the outer shell relative to that of the inner shell.

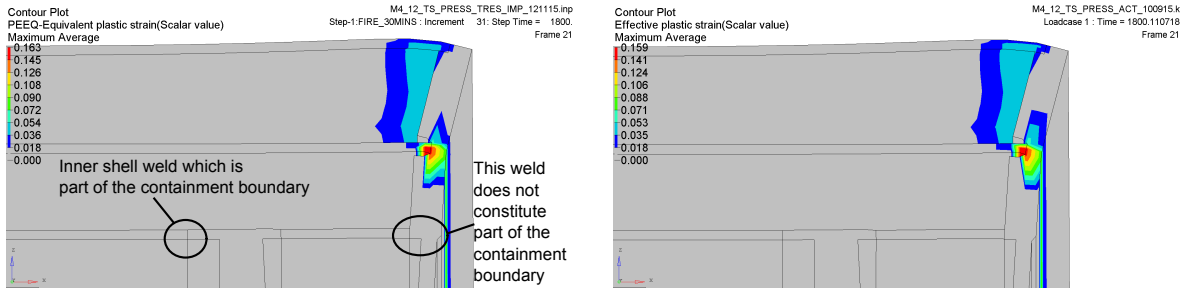

(a) Abaqus **(b) LS DYNA**

Figure 11: Effective Plastic Strain Contour Plots of Outer/Intermediate Shell to Base Plate Weld after 30 minutes

The outer shell is hottest in between the two trunnion reinforcing rings and therefore more susceptible to failure due to its lower mechanical properties between 600°C - 700°C. **Figure 12** shows the plastic strain contour plots predicted in the outer shell after 30 minutes (no further strain occurred during cooldown). The comparison is again in very good agreement; each model predicting a maximum "pool" of plastic strain of 0.5%. This is low and unlikely to cause an outer shell rupture at 25 barg pressure.

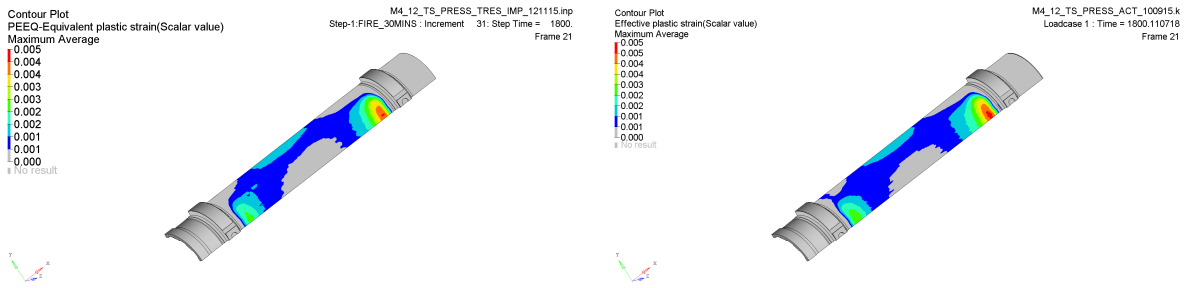

(a) Abaqus (Deformed Scale x1) **(b) LS DYNA (Deformed Scale x1)**

Figure 12: Effective Plastic Strain Contour Plots of Outer Shell after 30 minutes

No plastic strain occurred in the inner shell, so maximum stresses were assessed. **Figure 12** shows the von Mises stress contour plots of the inner shell after 30 minutes. In this analysis this was the time at which the peak stress occurred. The results indicate a difference in magnitude of 11 MPa between the codes; 296 MPa (Abaqus) and 307 MPa (LS DYNA). However it is evident from the contours that the deformed shape was different between the models. In the LS

DYNA model the inner shell becomes oval, under the trunnions the inner shell presses down on the fuel basket ribs, whereas at 90° from this position the shell expands away from the ribs. The Abaqus model uniformly bulges away from the ribs, as the internal pressure struggles to overcome the thermal expansion which would cause the inner shell to buckle. This difference in behaviour was attributed to small variations in the temperature profile and further work proved it was inconsequential **[12]**.

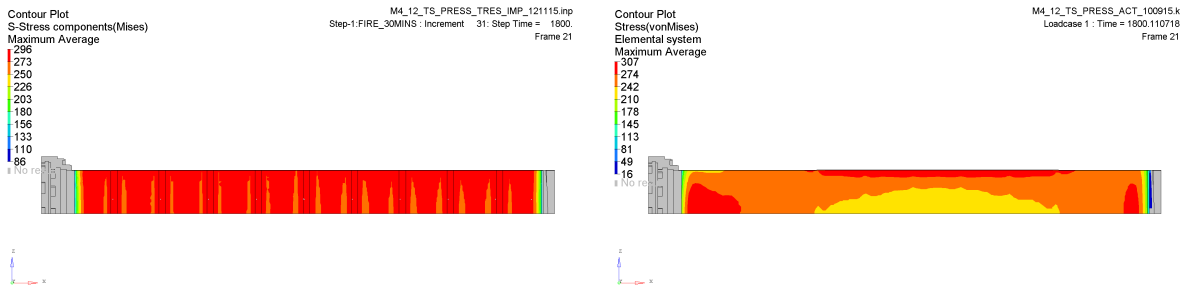

(a) Abaqus (Deformed Scale x1) **(b) LS DYNA (Deformed Scale x1)**

Figure 13: Von Mises Stress Contour Plots of Inner Shell after 30 minutes

Discussion

As alluded to throughout this paper the study was finalised using more advanced techniques in Abaqus to solve hypothetical load cases with increasing pressures and initial shell imperfections. The addition of imperfections to the models introduced the main challenge for obtaining completed solutions.

In LS DYNA attempts to solve the highly non-linear snap-through behaviour of the shells was attempted with an automatic implicit-explicit switching method **[17, 18]**. This offered the advantage of maintaining large time steps with the implicit solver up to the point of instability and then switching to the explicit solver. Difficulties were experienced when switching back to the implicit solver which repeatedly failed to converge. Different strategies were attempted to control how long the solution spends solving in explicit mode and when to switch from implicit to explicit. However the process became very time consuming to achieve a set of solution parameters which reliably completed for multiple sensitivity studies.

Table 1: Analysis Run Times

Analysis Type	Abaqus Run Times	LS DYNA Run Times
Heat Transfer	3 hrs and 22 mins	5 hrs and 18 mins
Thermal Stress (Implicit)	9 hrs and 4 mins	15 hrs and 44 mins
Thermal Stress (Explicit)	56 hrs and 25 mins	N/A

However reliable solutions were achieved consistently using Abaqus/Explicit. This also required some trial and error when selecting a suitable termination time. Initial tests at compressing the full fire and cooldown into a time period of 10ms and 100ms indicated that the solution contained erroneous dynamic effects. The final time duration selected was 0.5 seconds per step (i.e. 500ms fire and 500ms cooling). This is a long time period for an explicit solution and causes significant overhead in analysis run time.

Table 1 shows the run times for the models presented here. The Abaqus implicit jobs were executed in shared memory mode on 6 CPUs, whereas the LS DYNA jobs were executed in shared memory on 12 CPUs. The Abaqus implicit jobs ran more efficiently (faster and with fewer CPUs) although the number of CPUs selected for the LS DYNA jobs may have actually slowed down the solution. The final runs were carried out using Abaqus/Explicit using 8 CPUs. These runs took significantly longer, so the final studies were a trade-off between tuning the implicit solver to run, which in itself is time consuming, or waiting for the explicit solver to complete.

Conclusions

New thermal stress analysis of the M4-12 package during a regulatory pool fire has been carried out to assess the possibility of internal pressure build up causing an inner shell failure due to off-gassing Vitrite. The conclusions of the overall study were that the inner shell will not fail before the outer shell, consequently the package containment boundary remains intact. This paper has presented preliminary work comparing the solution methods and techniques to solve the problem using both Abaqus and LS DYNA.

It was concluded that both codes are capable of solving transient heat transfer and thermal stress problems for RAM transport packages. Abaqus/Standard (implicit) appears to offer benefits in terms of speed of solutions and variety of methods available for this class of problem, however

LS DYNA has merits in its ease of use. In particular the ability to switch between implicit and explicit mode “on the fly” is promising.

There is a great deal of benefit in solving highly non-linear models simultaneously in two codes as it increases confidence in the solutions and understanding of the problem. With such a large number of potential methods available between the codes, the approach adopted was to use a process of elimination to find the most expedient solution path.

References

[1] S.F. Jagger, 2014, ”INS3578: IAEA 800°C Thermal Test - Report of the Repeat Test”, MH/14/11, Health and Safety Laboratory

[2] Chris Fry, 2016, ”Finite Element Analysis of Vitrite Pyrolysis Tests”, IN001252, Issue 1, AMEC Foster Wheeler

[3] Abaqus version 6.13.1, Simulia

[4] LS DYNA, version 6.1.1, LSTC

[5] BS EN 10088-1, 1995, ”Stainless Steels - Part 1: List of Stainless Steels”

[6] ASME II, 2013, Part D

[7] T. Roberts, 2001, ”The Properties of Balsa Wood used for Transport Flask Shock Absorbers”, RAT 293, Issue 1

[8] BS EN 755-2, 1997, ”Aluminium and Aluminium Alloys - Mechanical Properties”

[9] T. Roberts, 2001, ”The Properties of Natural Vitrite HTS Neutron Shielding Material”, RAT Report 3013

[10] J. Chen, B. Young, 2006, ”Stress-Strain Curves for Stainless Steel at Elevated Temperatures, Engineering Structures, 28, 1, 229-239,

[11] C. Fry, 2014, ”Good Practice Guide to Thermal Analysis and Testing of Transport Packages”, TCSC 1093, Transport of Radiactive Material Code of Practice

[12] A.Cummings, 2016, ”Technical Report - FEA Assessment of the Structural Integrity of the Inner Shell of the M4-12 when Subjected to a Regulatory Thermal Accident”, INS/ENG/R/15/205

[13] J.P. Holman, 2001, ”Heat Transfer”, New York, Eighth SI Metric, McGraw Hill

[14] J. Carvill, 1993, ”Mechanical Engineers Databook”, Elsevier, First Edition, IMechE

[15] P.Jacob, L. Goulding, 2002, ”An Explicit Finite Element Primer”, NAFEMS

[16] Altair Hyperworks Version 13.0.210

[17] A. Jonsson, 2015, DYNAMore, ”Some Guidelines for Implicit Analyses using LS DYNA”

[18] T. Borrvall, DYNAMore, Sweden, ”A guide to solving Implicit Mortar Contact Problems in LS DYNA”